



UNIVERSIDADE ESTADUAL DE CAMPINAS
SISTEMA DE BIBLIOTECAS DA UNICAMP
REPOSITÓRIO DA PRODUÇÃO CIENTÍFICA E INTELLECTUAL DA UNICAMP

Versão do arquivo anexado / Version of attached file:

Versão do Editor / Published Version

Mais informações no site da editora / Further information on publisher's website:

<https://ieeexplore.ieee.org/document/9079669>

DOI: 10.1109/tpwr.2020.2990968

Direitos autorais / Publisher's copyright statement:

©2020 by Institute of Electrical and Electronics Engineers. All rights reserved.

DIRETORIA DE TRATAMENTO DA INFORMAÇÃO

Cidade Universitária Zeferino Vaz Barão Geraldo

CEP 13083-970 – Campinas SP

Fone: (19) 3521-6493

<http://www.repositorio.unicamp.br>

Development of a Voltage-Dependent Line Model to Represent the Corona Effect in Electromagnetic Transient Program

Thassio Matias Pereira and Maria Cristina Tavares, *Senior Member, IEEE*

Abstract--This paper describes a new method to represent single-phase overhead transmission lines (TL) under corona effect in electromagnetic transient simulation program. Based on Bergeron model and the scheme proposed by Dommel to represent transmission lines in Electromagnetic Transients Programs (EMT), a voltage-dependent line model (VDLM) was developed. This model can be represented through of an equivalent impedance network and easily combined with other components of the electric power system. To solve the nodal equations of the network a simple technique is proposed, which is suitable to calculate lightning overvoltages transients and avoids the necessity of iterative methods, increasing the efficiency of the algorithm. The proposed method was implemented in Matlab software, and the simulation's results were compared with field measurements to verify the accuracy of the model. Comparisons were also made with the traditional linear Corona Model. A good agreement could be observed between them.

Index Terms-- Corona, Transmission line modeling, lightning overvoltages.

I. INTRODUCTION

Accurate knowledge of overvoltages' magnitude and waveform is essential to the insulation coordination design of overhead transmission lines. This information is normally obtained through digital simulations, where the Electromagnetic Transient Programs (EMT-type programs) are widely used due their versatile to represent several components of an electric power system.

The basic structure of the EMT was firstly presented by Dommel in 1969 [1]. Nowadays these programs have very robust line models capable of representing with good accuracy the frequency-dependence of line parameters [2], [3], [4], although the corona effect cannot be represent directly in these line models.

The corona effect occurs in an overhead line when the electric field in the conductor's surface exceeds a certain critical value, causing the ionization of the air and the generation of space charge in the vicinity of the conductor [5], [6]. This phenomenon acts as a natural attenuator of surges, reducing the magnitude of the overvoltages and slowing the traveling waves' propagation speed. For this reason, neglecting it on the simulations can lead to

This work was supported by the research agencies CAPES (code-001), CNPq (306351/2017-0) and FAPESP (2018/04174-7; 2017/20010-1). (Corresponding author: Thassio M. Pereira).

T. M. Pereira and M. C. Tavares are with School of Electrical and Computer Engineering, University of Campinas, Campinas, São Paulo 13083-852, Brazil (e-mail: tmatias@dsce.fee.unicamp.br; ctavares@unicamp.br).

unrealistic and conservative results [7]. However, since it has distributed, nonlinear, hysteretic and frequency-dependent behavior, the representation of corona effect in the electromagnetic transient simulations is not easy to perform.

To the best of the authors' knowledge, the only way to represent the corona effect in EMT consists in subdividing the TL into linear sections, and at each junction node is placed a shunt corona branch [8], [9]. Basing on this method, a technique that considers the corona branch implicitly was posteriorly proposed, it uses a recursive scheme and represents the line as a nonlinear component [10], [11]. Anyway, in these cases the corona is treated as an external and lumped component, and line parameters are kept invariant. To represent the distributed nature of the corona effect different methods were proposed over the years, which normally use numerical algorithms to solve the telegraph's equations [12], [13] or discretized Maxwell's equations [14], [15]. However, it should be noted that such methods are not suitable for representation in EMT type programs, since they are not described through Norton equivalents.

In this paper we present a new methodology to represent the corona effect in lightning overvoltages simulations. Basing on Bergeron line model and the scheme proposed by Dommel to represent single-phase overhead lines in EMT [1], a voltage-dependent line model (VDLM) was developed, which corresponds to a more general case of the Bergeron model and allows the corona effect to be represented directly into the line model. More specifically, the great difference between the proposed model and the previous models consists in the fact that the capacitance per unit of length of the line is treated as a voltage-dependent parameter, which results in a nonlinear representation of the line and reproduces the distributed nature of the phenomenon. Furthermore, since the VDLM can be represented by an equivalent impedance network, it can be implemented as a separate component or as a subroutine in any EMT program, which allows the model to be easily combined with other power system elements.

The corona model was implemented in Matlab software along with an algorithm that automatically makes the spatial discretization of the line, besides it calculates the nodal voltages without using iterative methods, increasing the proposed model efficiency. Furthermore, to investigate its accuracy, comparisons between computed results and two different measurement data available in literature were carried out. Additional tests were made with traditional linear component method (TLCM). Good agreement was obtained for both cases.

This paper is structure as follows. The first part of the document presents a brief review of the classical Bergeron line model.

The second part describes the structure of the VDLM, the corona model and the computational procedure. The third part validates the proposed method.

II. A REVIEW OF BERGERON LINE MODEL

Consider a lossless single-phase transmission line with constant parameters (CP) and length l , as shown in Fig. 1. According to Bergeron model, the relationship between voltage and current at the terminals k and m can be expressed by (1) and (2).

$$v_k(t) + Z_0 \cdot (-i_{k,m}(t)) = v_m(t - \tau_0) + Z_0 \cdot i_{m,k}(t - \tau_0) \quad (1)$$

$$v_m(t) + Z_0 \cdot (-i_{m,k}(t)) = v_k(t - \tau_0) + Z_0 \cdot i_{k,m}(t - \tau_0) \quad (2)$$

Where:

$$Z_0 = \sqrt{\frac{L_0}{C_0}} \quad (3)$$

$$\tau_0 = \frac{l}{v_{prop}} = \sqrt{L_0 C_0} \cdot l \quad (4)$$

In above equations, $i_{k,m}(t)$ and $i_{m,k}(t)$ correspond to the instantaneous currents entering terminals k and m , respectively; $v_k(t)$ and $v_m(t)$ correspond to the instantaneous voltages on the terminals k and m , respectively, Z_0 is the characteristic impedance of the line, τ_0 is the travel time (or the time that a signal takes to travel from one terminal to the other), v_{prop} is the wave propagation speed, L_0 and C_0 are, respectively, the series inductance and the shunt capacitance of the line per unit of length.

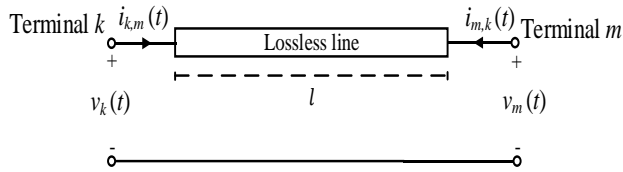


Fig. 1. Lossless single-phase line with constant parameters.

Equations (1) and (2) may be properly understood as follows: a signal that leaves a line terminal reaches the other end with the same amplitude (lossless line), after a time delay of τ_0 . This concept is shown in Fig. 2.

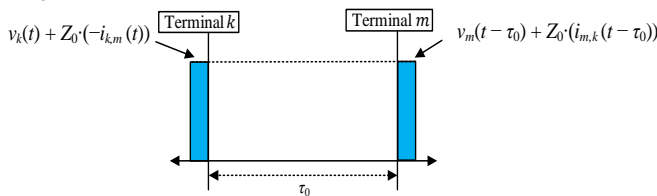


Fig. 2. Graphical interpretation of the Bergeron's equations for a lossless single-phase line.

By means of (1) and (2) we can obtain (5) and (6), which describe the currents at line terminals, $i_{k,m}(t)$ and $i_{m,k}(t)$. This pair of equations can also be expressed by an equivalent impedance network, which is composed by resistors and historical current sources, as shown in Fig. 3.

$$i_{k,m}(t) = \frac{v_k(t)}{Z_0} + I_k(t - \tau_0) \quad (5)$$

$$i_{m,k}(t) = \frac{v_m(t)}{Z_0} + I_m(t - \tau_0) \quad (6)$$

$$I_k(t - \tau_0) = -\frac{v_m(t - \tau_0)}{Z_0} - i_{m,k}(t - \tau_0) \quad (7)$$

$$I_m(t - \tau_0) = -\frac{v_k(t - \tau_0)}{Z_0} - i_{k,m}(t - \tau_0) \quad (8)$$

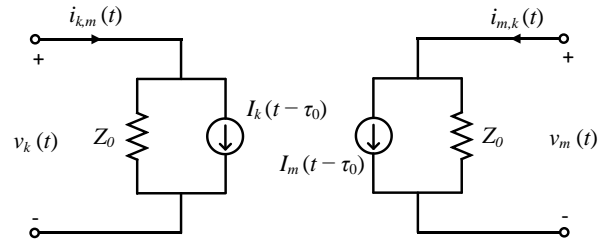


Fig. 3. Equivalent impedance network of the lossless Bergeron single-phase line model.

To calculate the currents $i_{k,m}(t)$ and $i_{m,k}(t)$ it is necessary to know the voltages at line terminals, $v_k(t)$ and $v_m(t)$. These voltages can be calculated by means of the system nodal equations, as shown in (9):

$$[Y] \cdot [v(t)] = [i(t)] - [I] \quad (9)$$

Where:

$[Y]$ - Nodal conductance matrix

$[v(t)]$ - Column vector of node voltages at time t . Some elements may be known (specified voltage source from datum node), and others are unknown.

$[i(t)]$ - Column vector of injected node currents at time t (specified current sources from datum to node)

$[I]$ - Known column vector, which is made up from equivalent historical currents sources.

Since (9) corresponds to a system of linear equations it can be easily solved by different methods, which are well-known and will not be explained here. More information can be found in [1], [16].

III. VOLTAGE-DEPENDENT LINE MODEL

To represent the corona effect in transmission lines we can consider that the shunt capacitance and shunt conductance in any point along the line are voltage dependent, which means that the distributed characteristic of this phenomenon should be properly modeled. Thereby, the only way to represent this phenomenon is through spatial discretization.

The appropriate length of each line section when performing the spatial discretization depends on the type of the phenomenon analyzed. By performing the discretization of the line and calculating the shunt capacitance and shunt conductance based on the voltage at each line section terminal, it is assumed that the voltage along the line section is constant. However, this approximation is reasonable only if the travel time along the section is a fraction of the period associated to the maximum frequency involved in the analysis. For lightning, for example, the maximum frequency involved in the analysis is in the range of 1 MHz, which is equivalent to a period of 1 μ s. Since the surge waves propagate less than

300 m each microsecond, section lengths must be of 50 m or less [8].

Assuming that the line has been properly discretized according to the analyzed phenomenon, the voltage along a section is approximately the same. Thus, the shunt capacitance and shunt conductance can be calculated based on the voltage at sending end $v_k(t)$ or receiving end $v_m(t)$, which will generically be named $v(t)$ in the next sections.

A. Representation of Dynamic Capacitance

Consider again the lossless transmission line at Fig. 1. To represent the dynamic capacitance it is necessary to consider the characteristic impedance and the travel time as voltage functions, as shown in (10) and (11):

$$Z(v(t)) = \sqrt{\frac{L_0}{C(v(t))}} \quad (10)$$

$$\tau(v(t)) = \sqrt{L_0 \cdot C(v(t))} \cdot l \quad (11)$$

Thus, (1) and (2) can be rewritten as shown in (12) and (13):

$$\begin{aligned} v_k(t) + Z(v(t)) \cdot (-i_{k,m}(t)) \\ = v_m(t - \tau(v(t))) + Z(v(t)) \cdot i_{m,k}(t - \tau(v(t))) \end{aligned} \quad (12)$$

$$\begin{aligned} v_m(t) + Z(v(t)) \cdot (-i_{m,k}(t)) \\ = v_k(t - \tau(v(t))) + Z(v(t)) \cdot i_{k,m}(t - \tau(v(t))) \end{aligned} \quad (13)$$

Knowing that when the TL is under corona effect a rise in the shunt capacitance occurs, it can be seen in (10) and (11) that the phenomenon causes simultaneously a decreasing in characteristic impedance and an increasing in the travel time.

A physical interpretation of (12) and (13) is shown in Fig. 4. As can be seen, these equations describe that when a signal leaves a line terminal it gets to the other end with the same amplitude (lossless). However, differently from (1) and (2), in this case the signal amplitude and the travel time are voltage dependent and can be modified in each time step, following $v(t)$.

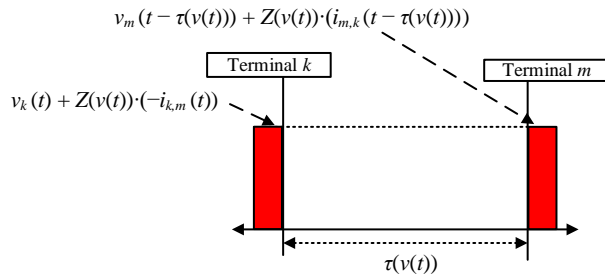


Fig. 4. Graphical interpretation of the Bergeron's equations for a lossless line with representation of the dynamic capacitance.

Isolating $i_{k,m}(t)$ and $i_{m,k}(t)$ in (12) and (13) we obtain (14) and (15), respectively, which describe the currents on each terminal of a lossless TL with voltage-dependent capacitance. These pair of equations also can be represented by an equivalent impedance network as shown in Fig. 5, which is

composed by non-linear resistors and voltage-dependent current sources.

$$i_{k,m}(t) = \frac{v_k(t)}{Z(v(t))} + I_k(t - \tau(v(t))) \quad (14)$$

$$i_{m,k}(t) = \frac{v_m(t)}{Z(v(t))} + I_m(t - \tau(v(t))) \quad (15)$$

$$I_k(t - \tau(v(t))) = -\frac{v_m(t - \tau(v(t)))}{Z(v(t))} - i_{m,k}(t - \tau(v(t))) \quad (16)$$

$$I_m(t - \tau(v(t))) = -\frac{v_k(t - \tau(v(t)))}{Z(v(t))} - i_{k,m}(t - \tau(v(t))) \quad (17)$$

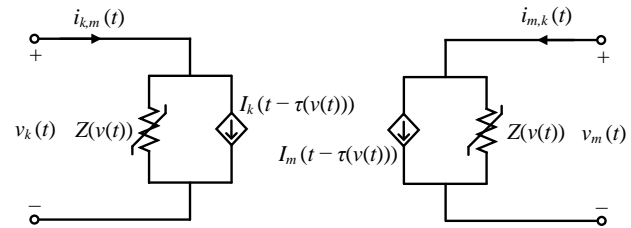


Fig. 5. Equivalent impedance network of a lossless TL with representation of dynamic capacitance.

B. Representation of series resistance and shunt conductance

The shunt conductance and series resistance can be represented by means of lumped resistances combined with the lossless line. Since short line sections are used to represent the corona effect in electromagnetic transients, these parameters can be included only in the line terminals [10], as shown in Fig. 6(a). In this figure, R_l is the total series resistance of the section, and R_s is the total shunt resistance, which assumes very high values when the line is not under corona. It should be noted that since the shunt resistance is placed in parallel with the line terminals, it must be multiplied by two and not divided by two, as done for the series resistance.

The Fig. 6(a) circuit can be further simplified with Kirchoff's Laws, resulting in Fig. 6(b) circuit. The currents at the line terminals are described by (18) and (19).

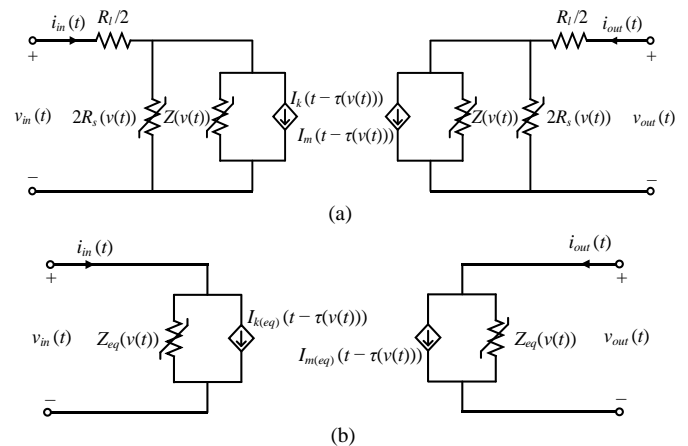


Fig. 6. TL equivalent impedance network with approximate representation of series losses, voltage-dependent capacitance and shunt conductance. (a) Complete circuit. (b) Simplified circuit.

$$i_{in}(t) = \frac{v_{in}(t)}{Z_{eq}(v(t))} + I_{k(eq)}(t - \tau(v(t))) \quad (18)$$

$$i_{out}(t) = \frac{v_{out}(t)}{Z_{eq}(v(t))} + I_{m(eq)}(t - \tau(v(t))) \quad (19)$$

Where:

$$I_{k(eq)}(t - \tau(v(t))) = -\frac{1}{Z_{eq}(v(t))} \cdot \left[v_{out}(t - \tau(v(t))) + \left(Z_s(v(t)) - \frac{R_l}{2} \right) \cdot i_{out}(t - \tau(v(t))) \right] \quad (20)$$

$$I_{m(eq)}(t - \tau(v(t))) = -\frac{1}{Z_{eq}(v(t))} \cdot \left[v_{in}(t - \tau(v(t))) + \left(Z_s(v(t)) - \frac{R_l}{2} \right) \cdot i_{in}(t - \tau(v(t))) \right] \quad (21)$$

$$Z_s(v(t)) = \frac{2R_s(v(t)) \cdot Z(v(t))}{2R_s(v(t)) + Z(v(t))} \quad (22)$$

$$Z_{eq}(v(t)) = Z_s(v(t)) + \frac{R_l}{2} \quad (23)$$

Some important considerations must be made in relation to (18) and (19):

- It can be observed that these equations consist of a more general case of Bergeron Model. Calculating the limit when $R_s(v(t)) \rightarrow \infty$, $R_l \rightarrow 0$, $Z_{eq}(v(t)) \rightarrow Z_0$, $\tau(v(t)) \rightarrow \tau_0$ we obtain (5) and (6), which represent the currents at the terminals of a lossless TL. Thus, this equations can be used in general, both when the corona effect occurs as when there is no occurrence of the phenomenon.
- Variations on capacitance are represented in the equivalent impedance $Z_{eq}(v(t))$ and in the travel time $\tau(v(t))$. The value of these parameters can be updated every time step, however, the variation must be smooth, otherwise numerical oscillations may occur.
- As the travel time $\tau(v(t))$ varies with the voltage, in general it will not be an integer of the time step used in the simulation. This will imply in applying linear interpolation to the variables $I_{k(eq)}$ and $I_{m(eq)}$, as done in EMT-type programs to represent frequency-dependent transmission lines [4].

C. Corona model

To calculate the voltage-dependent capacitance and shunt conductance the empirical equations proposed by Skilling [17] and Umoto [18] were adopted. This model is adequate since the capacitance variation proposed is smooth and without discontinuity points. Moreover, it has already been adopted in previous works of lightning overvoltages calculation ([19] - [20]) with satisfactory results, although it does not consider the frequency-dependence of corona phenomenon.

According to the Skilling-Umoto model, the capacitance per unit of length and total shunt resistance of a section with length d can be obtained, respectively, by (24) and (26).

$$C(v(t)) = \begin{cases} C_0, & v(t) < V_{crit} \\ C_0 + 2K_C \left(1 - \frac{V_{crit}}{v(t)} \right), & v(t) \geq V_{crit} \end{cases} \quad (24)$$

$$G(v(t)) = \begin{cases} 0, & v(t) < V_{crit} \\ K_G \left(1 - \frac{V_{crit}}{v(t)} \right)^2, & v(t) \geq V_{crit} \end{cases} \quad (25)$$

$$R_s(v(t)) = \frac{1}{G(v(t)) \cdot d} \quad (26)$$

$$K_C = \sigma_C \sqrt{\frac{r}{2h}} \cdot 10^{-11} \text{ F/m} \quad (27)$$

$$K_G = \sigma_G \sqrt{\frac{r}{2h}} \cdot 10^{-11} \text{ S/m} \quad (28)$$

Where:

$v(t)$: Line voltage [V]

V_{crit} : Corona onset voltage (or critical voltage) [V]

r ; h : Radius and height above ground of conductor [m], respectively

σ_C ; σ_G : Corona loss constants in [F/m] and [S/m], respectively.

D. Computational procedure

As can be seen in (18) and (19), it is necessary to know the voltages at the line terminals to calculate the currents $i_{in}(t)$ and $i_{out}(t)$. As shown in section II, nodal equations were used to calculate these voltages. However, it can be observed in Fig. 6(b) that the equivalent conductances and the historical currents in equivalent impedance network are voltage functions, which makes the nodal conductance matrix and the historical currents vector also functions of the voltage, as shown in (29):

$$[\mathbf{Y}([\mathbf{v}(t)])] \cdot [\mathbf{v}(t)] = [\mathbf{i}(t)] - [\mathbf{I}([\mathbf{v}(t)])] \quad (29)$$

To solve (29) it is necessary to use iterative methods [1]. However, considering that the line must be discretized into a very large number of sections, the solution of all these equations has a high computational burden. To avoid this an approximation is adopted, where the nodal voltages $[\mathbf{v}(t)]$ are obtained using the nodal conductance matrix and the historical current vector calculated based on previous time step, as shown in (30).

$$[\mathbf{Y}([\mathbf{v}(t - \Delta t)])] \cdot [\mathbf{v}(t)] = [\mathbf{i}(t)] - [\mathbf{I}([\mathbf{v}(t - \Delta t)])] \quad (30)$$

As $[\mathbf{Y}([\mathbf{v}(t - \Delta t)])]$, $[\mathbf{i}(t)]$ and $[\mathbf{I}([\mathbf{v}(t - \Delta t)])]$ are known, the nodal voltages calculation consists in the resolution of a linear system. This procedure avoids the need of iterative methods, increasing the efficiency of the proposed algorithm. It should be noted that this approximation is valid because a very short time step is used for the lightning overvoltages simulation, actually of the order of ns. As a result the nodal voltages and the voltage-dependent conductances within the nodal conductance matrix vary smoothly from one time step to the next.

This solution technique is shown in the flow chart of Fig. 7, where the process of the line spatial discretization was automated. Some important algorithm properties are highlighted below:

- As shown in Fig. 8, the line is discretized into n sections of d length, and each line section is represented by the equivalent impedance network of Fig. 6(b). The travel time and the equivalent impedance are calculated based on the receiving end voltage of section (v_{out}^s), where $s = 1, 2, 3, \dots, n$.
- The automatic line discretization can be easily performed because the equivalent impedance network is composed only by one resistor connected to each terminal. Thus, the

transmission line can be represented by diagonal elements in the nodal conductance matrix [1].

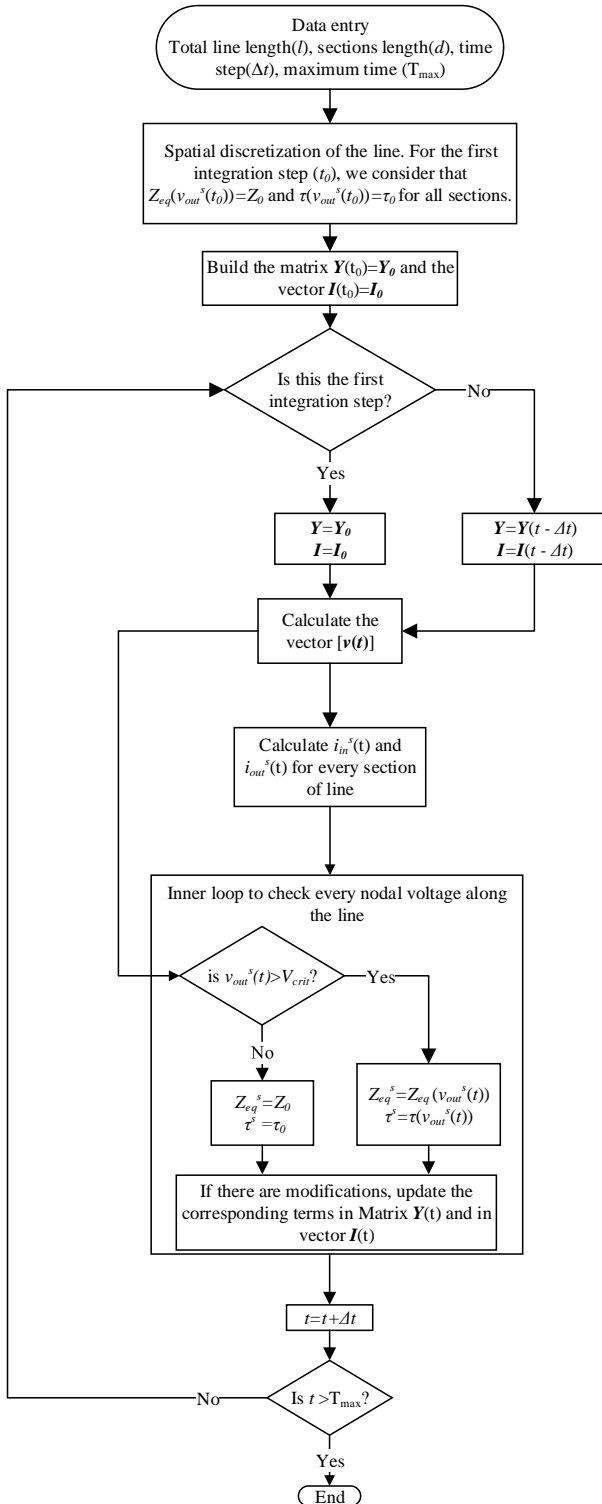


Fig. 7. Flow chart of the transient computation program.

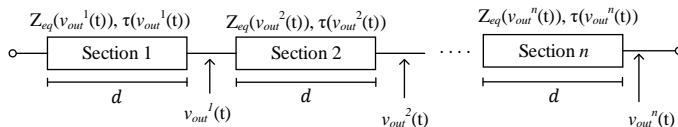


Fig. 8. Spatial line discretization.

- In the first time step no section of the line is considered under corona effect. Thus, $Z_{eq}^s = Z_0$ and $\tau^s = \tau_0$. This means that the nodal conductance matrix Y and the vectors of historical current I can be built as usual. For the next time steps these parameters are updated based on the voltage calculated in the previous time step.
- In the absence of the corona effect, the nodal conductance matrix is not modified. When the voltage across any line section becomes greater than the critical voltage (V_{crit}), the equivalent impedance and travel time of the section are recalculated, and the corresponding terms are updated in the matrix Y , as well as the historical current vectors I .

IV. VALIDATION TESTS

The proposed algorithm was implemented in Matlab software, and to evaluate its performance simulations were carried out and compared with two different field tests available in the literature.

In addition, the results obtained with the VDLM were also compared with the traditional linear component method (TLCM), normally used in simulations in EMT-type programs. As previously commented, this method consists in discretizing the transmission line into linear sections, and in each junction node is disposed a shunt bus that represents the corona effect according the corona model adopted (Fig. 9). In this paper, comparisons were made with the linear corona model proposed by Motoyama and Ametani [21]. This model is also based on the Skilling-Umoto equations, where the authors carry out an adaptation that allows it to be easily implemented in EMT-type programs. Simulations with this model were performed in PSCAD/EMTDC software, which has in its library all the necessary components for the model implementation. A more detailed description about the linear corona model can be found in Appendix A.

As the VDLM is not able to represent the frequency dependence of the line parameters, to make a fair comparison at this stage no frequency dependence was adopted. To circumvent this problem constant parameter model was adopted, and line series impedance was calculated for 100 kHz.

Finally, it should be noted that although these measurements were performed on three-phase transmission lines, they can be represented in the simulations as single-phase lines, because only one phase was energized. Adjacent phases did not interfere in the results. This procedure has already been adopted in previous studies [8], [10], [22], [23].

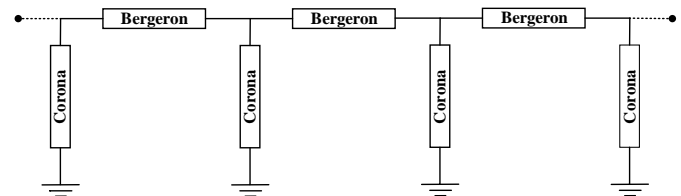


Fig. 9. Spatial discretization of the line applied in the TLCM.

A. Simulations for Tidd line experiments

In the early 50's, Wagner et al. carried out a series of experiments in the Tidd line to investigate the influence of the corona effect on lightning overvoltages propagation [24].

The scheme used to represent this line is presented in Fig. 10. The sending end is connected to a lumped voltage source, where a positive pulse voltage similar to double exponential of 1.55 MV peak (positive), 1 μ s rise time and 6.3 μ s time-to-half value is applied. The transmission line is composed by a 2.3-km-long overhead horizontal ACSR wire (25.40 mm radius), which is at an average height (H) of 18.89 m. The soil resistivity is 20 Ω ·m [23]. The receiving end is connected to a matching resistor, whose resistance is equal to the characteristic impedance of the line in the absence of corona (Z_0).

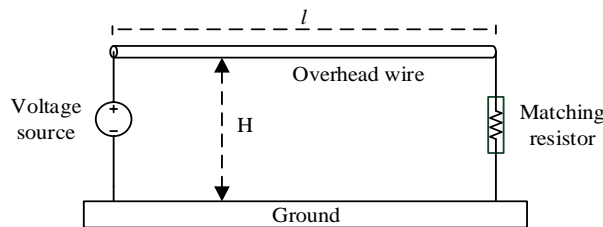


Fig. 10. Configuration used to represent the Tidd and Shiobara lines in the simulations.

In the Table I is shown the line parameters calculated for frequency $f = 100$ kHz, and in the Table II is shown the corona model parameters. It should be noted that the corona loss constants (σ_G and σ_C) were adjusted by a trial-and-error process in which simulations were carried out varying their values and the computed waveforms were compared with measurements.

An important observation must be made regarding the ideal values for the σ_G and σ_C constants, which are different for the TLCM and the VDLM. It occurs because these constants determine the value of the corona capacitance and shunt conductance. However, the circuit structure in each model is different, and therefore the values of the circuit components are also different. The adoption of different values for the σ_G and σ_C parameters does not affect the physical coherence of the models, since these parameters are only numeric values, which has no direct physical meaning.

To the simulations, for both TLCM and VDLM the line was discretized into 115 sections of 20 meters, and a time-step $\Delta t = 1$ ns was adopted. In Fig. 11(a) is shown the computed waveforms with the Bergeron model without representation of the corona effect, and in Fig. 11(b) is shown the results obtained with the TLCM and the VDLM. Simulations results are plotted with field measurements at approximately 660 m, 1300 m and 2180 m from sending end.

TABLE I
Tidd Line Parameters – 100 kHz

R_0 [Ω /m]	L_0 [μ H/m]	C_0 [pF/m]	Z_0 [Ω]
0.02	1.49	7.61	443.65

TABLE II
Corona Model Parameters for Tidd Line

	h [m]	r [mm]	σ_G [S/m]	σ_C [F/m]	V_{crit} [kV]
TLCM	18.89	25.40	$4.5 \cdot 10^6$	15	470
VDLM	18.89	25.40	$33 \cdot 10^9$	24	470

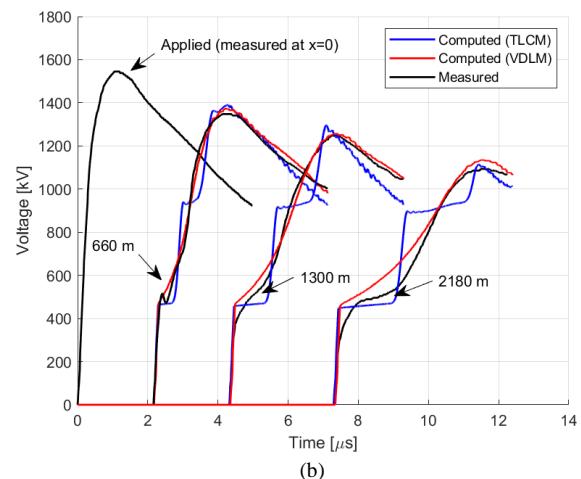
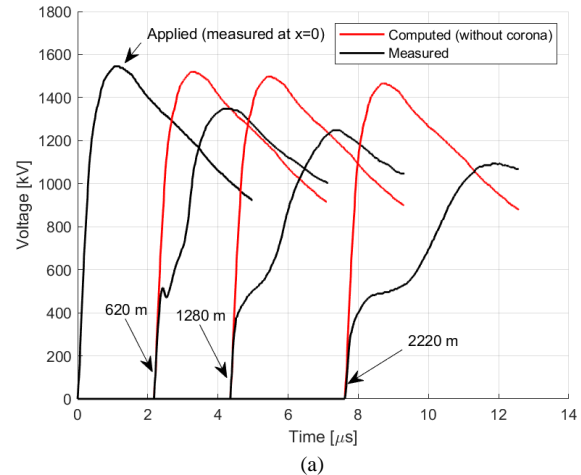


Fig. 11. Surge propagation on Tidd line. Comparison between measured and computed waveforms. (a) Bergeron without corona. (b) TLCM and VDLM.

B. Simulations for Shiobara line experiments

In this section it is introduced the configuration used in the simulations to reproduce the experiments on the Shiobara line, which were carried out by Inoue [25]. Similarly to the Tidd line experiments, the system can be represented by a lumped voltage source, a horizontal overhead wire and a matching resistor. The difference is that, in this case, it is applied a non-standard waveform of 1.58 MV peak (positive) with 1.2 μ s of rise time, and the line is composed by a 1.4-km-long overhead horizontal ACSR wire (12.65 mm radius), arranged 22.2 m above ground. The soil resistivity was taken as 100 Ω ·m, since it was not measured for the site where the experiments were performed. Tables III and IV show, respectively, the line parameters calculated for frequency $f = 100$ kHz and the corona model parameters.

TABLE III
Shiobara Line Parameters – 100 kHz

R_0 [Ω/m]	L_0 [$\mu H/m$]	C_0 [pF/m]	Z_0 [Ω]
0.04	1.66	7.05	499

TABLE IV
Corona Model Parameters for Shiobara Line

	h [m]	r [mm]	σ_G [s/m]	σ_C [F/m]	V_{crit} [kV]
TLCM	22.2	12.65	$13 \cdot 10^6$	12	303
VDLM	22.2	12.65	$15 \cdot 10^9$	27	303

For both TLCM and VDLM the line was discretized into 70 sections of 20 meters, and a time-step $\Delta t = 1$ ns was adopted. In Fig. 12(a) is shown the computed waveforms with the Bergeron model without representation of the corona effect, and in Fig. 12(b) is shown the results obtained with the TLCM and the VDLM. In both cases, the simulations results are plotted with field measurements at approximately 360 m, 700 m and 1060 m from sending end.

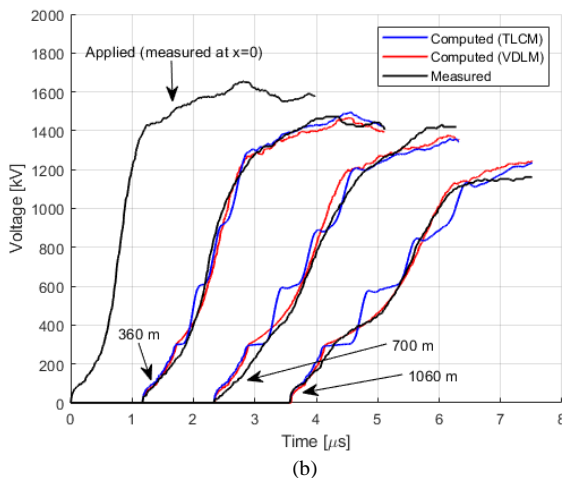
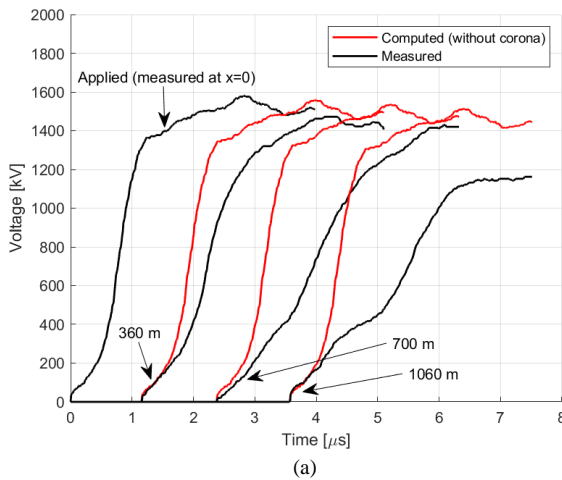


Fig. 12. Surge propagation on Shiobara line. Comparison between measured and computed waveforms. (a) Bergeron without corona. (b) TLCM and VDLM.

The Figs. 11(a) and 12(a) only confirm the well-known fact that disregarding corona effect in the simulations leads to very conservative results, and the attenuation and distortion increase as the signal propagates along the line. In this case, the maximum difference between measured and calculated

voltage peak is around 33% for the Tidd line and 30% for the Shiobara line.

On the other hand, Figs. 11(b) and 12(b) present comparisons between the results obtained with the TLCM, VDLM and field measurements. As can be seen, the waveforms produced by the VDLM have a good agreement with the measurements, being able to reproduce with a better precision level than the TLCM the attenuations and distortions caused by the corona effect. This occurs due to the fact that, as previously mentioned, in the VDLM the capacitance and shunt conductance of the line are represented as non-linear parameters, and for this reason the model is capable to accurately represent the real nature of the corona effect.

Regarding the computation time, it is worth noting that VDLM has a slightly longer calculation time than the TLCM. More specifically, in the case of simulations for Tidd line, where the line was discretized into 115 sections and a time-step $\Delta t = 1$ ns was adopted, the total simulation time to the VDLM was approximately 30 s, whereas the TLCM (performed in the PSCAD software) was approximately 20 s. It should be noted that all simulations were performed on a Dell XPS 8930 Desktop Computer, which was an Intel Core i7 processor and 16 GB RAM memory.

V. CONCLUSIONS

In the present document a voltage-dependent line model (VDLM) was introduced. It is a generalization of Bergeron line model and can represent the corona effect produced by lightning overvoltages simulations. Since the VDLM can be represented by an equivalent impedance network, it is possible to implement it in EMT-type programs. The main advantage of this model is that the corona effect can be directly incorporated in transmission line equations, and not as an external parameter.

The proposed model was tested with Matlab software along with an efficient algorithm that allows the automatic line discretization and solves the system through nodal equations without the use of iterative methods. To calculate the voltage-dependent shunt capacitance and shunt conductance, the Skilling-Umoto equations were adopted.

Validations tests were implemented considering surge propagation in two different transmission lines and compared with field measurements and the traditional linear component method. The simulations results validate the robustness of the VDLM, showing that it is capable of representing the corona effect with good accuracy and low computational cost.

In forthcoming material VDLM will be extended to incorporate the frequency-dependence of line parameters and to represent multiphase transmission lines.

VI. APPENDIX

A. Linear Corona Model

This section presents a brief review of the linear corona model adopted in this work, which was proposed by Motoyama and Ametani in 1987 [21]. In fact, this model consists of a piecewise linearization of the non-linear corona

model presented by K. Lee [19], which is in turn based on the Skilling-Umoto equations.

In this model, corona is represented by three parallel linear R-C branches, which are combined with diodes and DC voltage sources, as shown in Fig. 13. As commented in section IV, to represent the corona effect in EMT-type programs this circuit is arranged at each junction node of the line (Fig. 9). The parameters of the model can be calculated through equations (30) – (34).

$$V_1 = V_{crit} \quad V_2 = 2V_{crit} \quad V_3 = 3V_{crit} \quad (30)$$

$$R_k = \frac{1}{K_G \cdot \left[1 - \frac{V_{crit}}{V_{crit} + V_k}\right]^2} \cdot d \quad (31)$$

$$C_k = 2K_C \cdot \left[1 - \frac{V_{crit}}{V_{crit} + V_k}\right] \cdot d \quad (32)$$

$$K_G = \sigma_G \sqrt{\frac{r}{2h}} \cdot 10^{-11} \quad (33)$$

$$K_C = \sigma_C \sqrt{\frac{r}{2h}} \cdot 10^{-11} \quad (34)$$

In the above equations, C_k is the linear corona capacitance, in F; R_k is the linear corona resistance, in Ω ; V_{crit} is the corona onset voltage, in kV; r is the conductor radius, in m; h is the conductor height above ground, in m; d is the section length adopted in the line spatial discretization, in m; σ_G and σ_C are corona loss constants, in S/m and F/m, respectively; $k = 1,2,3$.

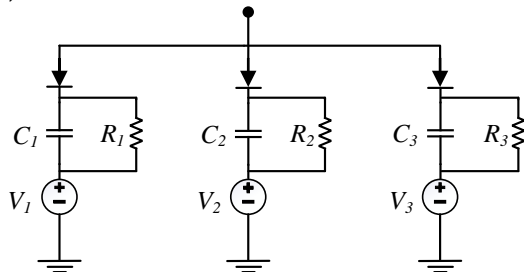


Fig. 13 – Linear corona model proposed by Motoyama and Ametani.

VII. ACKNOWLEDGMENT

The authors are grateful to Manitoba Hydro International Ltd for providing us with a professional PSCAD license during the development of this work.

VIII. REFERENCES

- [1] H. W. Dommel, "Digital Computer Solution of Electromagnetic Transients in Single- and Multiphase Networks," *IEEE Trans. Power Appar. Syst.*, vol. PAS-88, no. 4, pp. 388–399, 1969.
- [2] J. Marti, "Accurate Modelling of Frequency-Dependent Transmission Lines in Electromagnetic Transient Simulations," *IEEE Trans. Power Appar. Syst.*, vol. PAS-101, no. 1, pp. 147–157, Jan. 1982.
- [3] T. Noda, N. Nagaoka, and A. Ametani, "Phase domain modeling of frequency-dependent transmission lines by means of an ARMA model," *IEEE Trans. Power Deliv.*, vol. 11, no. 1, pp. 401–411, 1996.
- [4] A. Morched, B. Gustavsen, and M. Tartibi, "A universal

model for accurate calculation of electromagnetic transients on overhead lines and underground cables," *IEEE Trans. Power Deliv.*, vol. 14, no. 3, pp. 1032–1038, Jul. 1999.

- [5] J. J. Clade, C. H. Gary, and C. A. Lefevre, "Calculation of Corona Losses Beyond the Critical Gradient in Alternating Voltage," *IEEE Trans. Power Appar. Syst.*, vol. PAS-88, no. 5, pp. 695–703, May 1969.
- [6] C. Jesus and M. T. C. Barros, "Modelling of corona dynamics for surge propagation studies," *IEEE Trans. Power Deliv.*, vol. 9, no. 3, pp. 1564–1569, 1994.
- [7] M. Cervantes *et al.*, "Simulation of Switching Overvoltages and Validation With Field Tests," *IEEE Trans. Power Deliv.*, vol. 33, no. 6, pp. 2884–2893, Dec. 2018.
- [8] S. Carneiro and J. R. Marti, "Evaluation of corona and line models in electromagnetic transients simulations," *IEEE Trans. Power Deliv.*, vol. 6, no. 1, pp. 334–342, 1991.
- [9] Z. Anane, A. Bayadi, and N. Harid, "A dynamic corona model for EMTP computation of multiple and non-standard impulses on transmission lines using a type-94 circuit component," *Electr. Power Syst. Res.*, vol. 163, pp. 133–139, Oct. 2018.
- [10] S. Carneiro, J. R. Marti, H. W. Dommel, and H. M. Barros, "An efficient procedure for the implementation of corona models in electromagnetic transients programs," *IEEE Trans. Power Deliv.*, vol. 9, no. 2, pp. 849–855, Apr. 1994.
- [11] H. M. Barros, S. Carneiro, and R. M. Azevedo, "An efficient recursive scheme for the simulation of overvoltages on multiphase systems under corona," *IEEE Trans. Power Deliv.*, vol. 10, no. 3, pp. 1443–1452, Jul. 1995.
- [12] X.-R. Li, O. P. Malik, and Z.-D. Zhao, "Computation of transmission line transients including corona effects," *IEEE Trans. Power Deliv.*, vol. 4, no. 3, pp. 1816–1822, Jul. 1989.
- [13] K. Huang, X. Zhang, and S. Tao, "Electromagnetic Transient Analysis of Overhead lines Including Corona and Frequency Dependence Effects under Damped oscillation Surges," *IEEE Trans. Power Deliv.*, vol. 33, no. 5, pp. 2198–2206, 2018.
- [14] T. H. Thang *et al.*, "FDTD simulation of lightning surges on overhead wires in the presence of corona discharge," *IEEE Trans. Electromagn. Compat.*, vol. 54, no. 6, pp. 1234–1243, 2012.
- [15] T. H. Thang, Y. Baba, N. Nagaoka, A. Ametani, N. Itamoto, and V. A. Rakov, "FDTD simulations of corona effect on lightning-induced voltages," *IEEE Trans. Electromagn. Compat.*, vol. 56, no. 1, pp. 168–176, 2014.
- [16] F. H. Branin, "Computer methods of network analysis," *Proc. IEEE*, vol. 55, no. 11, pp. 1787–1801, 1967.
- [17] H. H. Skilling and P. de K. Dykes, "Distortion of traveling waves by corona," *Electr. Eng.*, vol. 56, no. 7, pp. 850–857, Jul. 1937.
- [18] J. Umoto and T. Hara, "Numerical analysing of line equations considering corona loss on single-conductor system," *Electr. Eng. Japan*, vol. 89, pp. 909–916, 1969.
- [19] K. Lee, "Non-Linear Corona Models in an

- Electromagnetic Transients Program (EMTP),” *IEEE Trans. Power Appar. Syst.*, vol. PAS-102, no. 9, pp. 2936–2942, Sep. 1983.
- [20] N. Nagaoka, H. Motoyama, and A. Ametani, “Lightning surge calculations including corona effects using a two-conductor model,” *Electr. Power Syst. Res.*, vol. 13, no. 1, pp. 31–41, Aug. 1987.
- [21] H. Motoyama and A. Ametani, “Development of a linear model for corona wave deformation and its effects on lightning surges,” *Electr. Eng. Japan*, vol. 107, no. 2, pp. 98–106, 1987.
- [22] J. L. Naredo, A. C. Soudack, and J. R. Marti, “Simulation of transients on transmission lines with corona via the method of characteristics,” *IEE Proc. - Gener. Transm. Distrib.*, vol. 142, no. 1, p. 81, 1995.
- [23] T. H. Thang *et al.*, “Lightning surges on an overhead wire in the presence of corona: FDTD simulation of Wagner *et al.*’s experiment,” in *2012 Asia-Pacific Symposium on Electromagnetic Compatibility*, 2012, pp. 845–848.
- [24] C. F. Wagner, I. W. Gross, and B. L. Lloyd, “High-Voltage Impulse Tests on Transmission Lines [includes discussion],” *Trans. Am. Inst. Electr. Eng. Part III Power Appar. Syst.*, vol. 73, no. 2, pp. 196–210, Apr. 1954.
- [25] A. Inoue, “Propagation Analysis of Overvoltage Surges with Corona Based Upon Charge Versus Voltage Curve,” *IEEE Trans. Power Appar. Syst.*, vol. PAS-104, no. 3, pp. 655–662, Mar. 1985.

IX. BIOGRAPHIES



Thassio Matias Pereira was born in Minas Gerais, Brazil, in 1994. He received the electrical engineering degree from the Federal University of São João del-Rei, Brazil, in 2017, and his M.Sc. Degree in 2019 at University of Campinas. He is currently a D.Sc. candidate at the same University. His research interests include high voltage engineering, electromagnetic transients, lightning and computer simulations of electric power systems.



Maria Cristina Tavares (SM’08) received the Electrical Eng. Degree from Federal University of Rio de Janeiro, Brazil, in 1984, the M.Sc. degree from COPPE/UFRJ, Rio de Janeiro, Brazil, in 1991, and the D.Sc. degree from UNICAMP, Campinas, Brazil, in 1998. She has provided consultation for engineering firms and she is currently an Associate Professor at the University of Campinas, where she has been since 2002. Her research interests include electromagnetic transients in power systems, arc modeling, long distance transmission and computer applications for transient analysis in power systems.